



Analysis of Elastic Scattering Angular Distributions of ${}^7\text{Li} + {}^{159}\text{Tb}$ Reaction with Various Nuclear Potentials

Murat AYGUN^{1,*}

¹Bitlis Eren University, Faculty of Arts and Sciences, Department of Physics, 13000, Bitlis, Turkey

Article Info

Received: 22/11/2017

Accepted: 09/04/2018

Keywords

Density distribution
Double folding model
Elastic scattering

Abstract

In this study, new measured angular distributions of the elastic scattering of ${}^7\text{Li}$ from ${}^{159}\text{Tb}$ at various incident energies are analyzed by using phenomenological and microscopic approaches. In phenomenological calculations, Woods-Saxon potentials are used. For microscopic approach, the real part of the optical potential is collected in two steps; real potential with M3Y together with an imaginary part in Woods-Saxon form and real and imaginary folding potentials. Three different density distributions of the ${}^7\text{Li}$ projectile are investigated while the double folding calculations are performed. The emphasis, in this work, is to study the impact of both different nuclear potentials and different density distributions on the elastic scattering of new measured experimental data of the ${}^7\text{Li} + {}^{159}\text{Tb}$ reaction. The results provide a good description of the experimental data.

1. INTRODUCTION

Elastic scattering is the simplest of nuclear reactions. Elastic scattering is a state unchanged both the projectile and the target nucleus internal energies. Angular distributions of elastic scattering of many nuclear reaction processes are described with convenient nucleus-nucleus potential. In this way, the optical model (OM) which has a complex nuclear potential is one of the most useful models. It is considered as the sum of the real and imaginary potentials [1]. The real and the imaginary parts of the OM can consist of different potential types which are used to describe various nuclear interaction states. In this context, the number of free parameters can increase the used potential number. As a result of this, the double folding model (DFM) to determine the real part of the optical potential is extensively evaluated in the elastic scattering process [1] and the number of free parameters are reduced. In the calculations of the DFM, the density distributions of the projectile and the target nuclei play a very important role. Therefore, the analysis of density distributions of nuclei is a current topic in the field of nuclear physics [2–4].

${}^7\text{Li}$ is one of important nuclei of nuclear physics. Recently, Patel et al. [5] have reported new experimental data of the elastic scattering of ${}^7\text{Li}$ on ${}^{159}\text{Tb}$ for different incident energies of 24, 26, 28, 30, 35, 40, and 44 MeV. They have analyzed the experimental data by using the OM and the continuum-discretized coupled-channels (CDCC) approach. They have reported that the potential parameters have shown unusual energy dependence behavior for their real and imaginary parts. We think that to make further theoretical calculations at near barrier energies will be important. In this respect, to research whether the fits to the new measured data of the ${}^7\text{Li} + {}^{159}\text{Tb}$ reaction can be improved with both different nuclear potentials and different density distributions will be the main aim of this work.

In the present work, the OM calculations are performed to analyze the angular distributions of ${}^7\text{Li} + {}^{159}\text{Tb}$ at different energies. For this purpose, three different nuclear potentials are applied. Firstly, phenomenological model with the volume Woods-Saxon (WS) potential for both the real and imaginary

*Corresponding author, e-mail: murata.25@gmail.com

parts is evaluated. Secondly, the real part is obtained with the DFM while the imaginary potential is taken as the volume WS type. Also, various densities of the ${}^7\text{Li}$ nucleus are investigated while all the theoretical calculations are conducted. Thus, the relationship between the density distributions is researched. Thirdly, the real and imaginary parts of the optical potential are taken as folded potential.

The following section presents the methods applied in the theoretical calculations. Section 3 gives the results of the study. Section 4 shows a summary and conclusions of our work.

2. FORMALISM

2.1. Phenomenological Model

The nucleus-nucleus total interaction potential is considered as

$$U_{\text{total}}(r) = U_{\text{Coulomb}}(r) + \underbrace{-V_R f_1(R) - iW_V f_2(R)}_{U_{\text{Nuclear}}(r)} \quad (1)$$

The Coulomb potential [6] is approved as

$$U_{\text{Coulomb}}(r) = \frac{1}{4\pi\epsilon_0} \frac{Z_P Z_T e^2}{r}, \quad r \geq R_C$$

$$= \frac{1}{4\pi\epsilon_0} \frac{Z_P Z_T e^2}{2R_C} \left(3 - \frac{r^2}{R_C^2} \right), \quad r < R_C$$

$$R_C = 1.25(A_P^{\frac{1}{3}} + A_T^{\frac{1}{3}}) \quad (2)$$

The nuclear potential has the radial form factors, $f_i(R)$, shown by

$$f_i(R) = [1 + \exp(\frac{R - R_i}{a_i})]^{-1}, \quad R_i = r_i(A_P^{\frac{1}{3}} + A_T^{\frac{1}{3}}), \quad i = 1, 2 \quad (3)$$

This process is marked as WSP.

2.2. Double Folding Model

The DFM is applied to get the real part of the optical potential describing the nucleus-nucleus interaction. The double folding (DF) is given by

$$V_{\text{DF}}(r) = \int dr_1 \int dr_2 \rho_P(r_1) \rho_T(r_2) v_{NN}(r_{12}), \quad (4)$$

where $\rho_P(r_1)$, $\rho_T(r_2)$ and v_{NN} are the density distributions of projectile (${}^7\text{Li}$) and target (${}^{159}\text{Tb}$) and effective nucleon-nucleon interaction potential, respectively. For a comparative study, three type densities of ${}^7\text{Li}$ have been used. They are Variational Monte Carlo (VMC), Fermi (2pF) and Harmonic Oscillator (HO) density distributions. The density of ${}^{159}\text{Tb}$ has been obtained from RIPL-3 [7]. All the densities have been presented in comparison form in Figure 1.

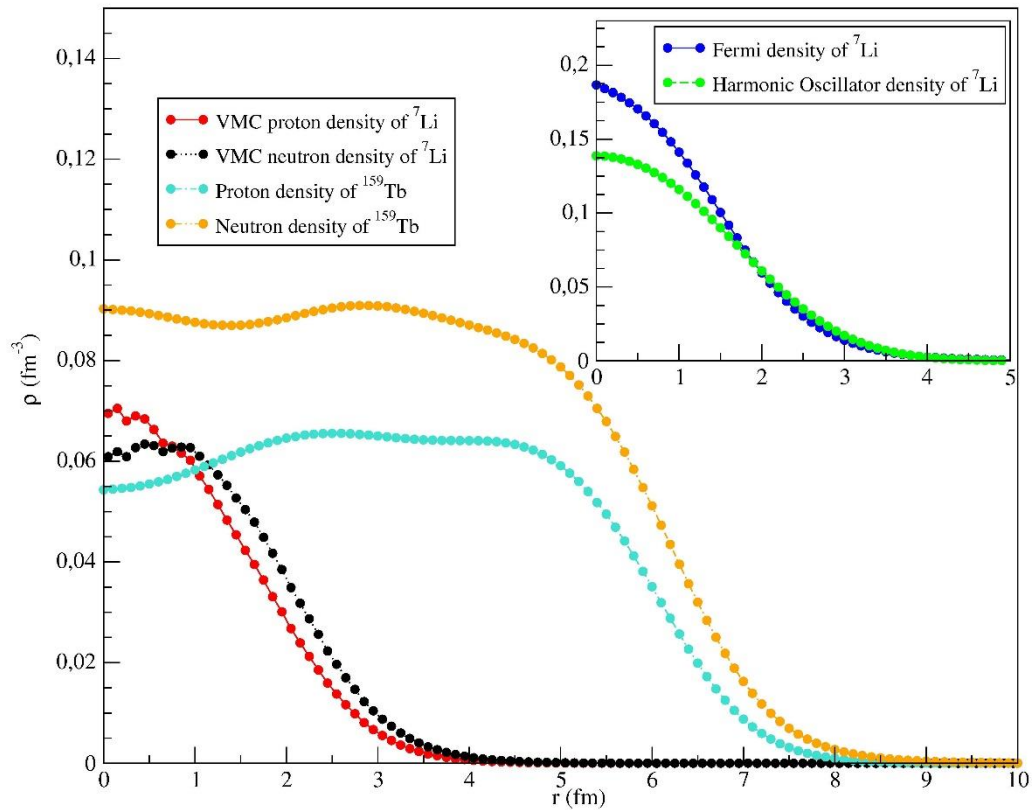


Figure 1. Density distributions in linear scale for ${}^7\text{Li}$ and ${}^{159}\text{Tb}$ nuclei

Several expressions for the v_{NN} can be found from literature. In our study, the Michigan 3 Yukawa (M3Y) [8] is used, which is presented by

$$v_{NN}(r) = 7999 \frac{\exp(-4r)}{4r} - 2134 \frac{\exp(-2.5r)}{2.5r} + J_{00}(E)\delta(r) \text{ MeV}, \quad (5)$$

where $J_{00}(E)$ is assumed as the exchange term given by

$$J_{00}(E) = 276 \left[1 - 0.005 \frac{E}{A_p} \right] \text{ MeV fm}^3 \quad (6)$$

As the imaginary potential, a four-parameter volume absorption potential of the WS has been used. It is parametrized by

$$W(r) = - \frac{W_0}{1 + \exp\left(\frac{r - R_W}{a_W}\right)} \quad (7)$$

where $R_W = r_W (A_p^{\frac{1}{3}} + A_T^{\frac{1}{3}})$. The presentation of this potential in our work is made as DF(R).

Finally, both real and imaginary parts are treated as folding potentials. For this, the imaginary potential is multiplied by a normalization factor (N_I). Thus, the ${}^7\text{Li} + {}^{159}\text{Tb}$ reaction can be written as

$$U_{\text{total}}(r) = U_{\text{Coulomb}}(r) - (N_R + N_I)V_{\text{DF}}(r) \quad (8)$$

This nuclear potential in our study is attributed to DF(R+I). While the theoretical calculations are performed, the codes FRESKO [9] and DFPOT [10] are used.

2.3. Nuclear Density Distributions

Here, three different densities of the ${}^7\text{Li}$ nucleus have been investigated. The DFM calculations via these densities have been performed.

2.3.1. Variational Monte Carlo (VMC) Density Distribution

The first density of the ${}^7\text{Li}$ nucleus in obtaining nuclear potential is the Variational Monte Carlo (VMC) density distribution. It is calculated by using the Argonne v18 (AV18) two nucleon and Urbana X three-nucleon potentials (AV18+UX) reported in Ref. [11].

2.3.2. Fermi (2pF) Density Distribution

The second density of the projectile is in the two-parameter Fermi (2pF) density form formulated as

$$\rho(r) = \frac{\rho_0}{1 + \exp\left(\frac{r-c}{z}\right)}, \quad (9)$$

where $\rho_0=0.2006$, $c=1.501$ and $z=0.578$ [12].

2.3.3. Harmonic Oscillator (HO) Density Distribution

The third density used for ${}^7\text{Li}$ in our work is the harmonic oscillator (HO) density in the following form

$$\rho(r) = (\xi + \gamma r^2) \exp(-\beta r^2) \quad (10)$$

where $\xi=0.1387$, $\gamma=0.0232$ and $\beta=0.3341$ [13].

2.4. Volume Integrals

The volume integrals determined from the theoretical analysis of the reaction investigated can be evaluated in examining the relation between the real and imaginary potentials. They are assumed as the real (J_V) and imaginary (J_W) volume integrals. In this respect, the J_V volume integral is written as

$$J_V(E) = \frac{4\pi}{A_p A_T} \int V(r, E) r^2 dr, \quad (11)$$

and the J_W volume integral is

$$J_W(E) = \frac{4\pi}{A_p A_T} \int W(r, E) r^2 dr. \quad (12)$$

2.5. χ^2 Value

The χ^2 value is generated by

$$\chi^2 = \frac{1}{N} \sum_{i=1}^N \frac{(\sigma_{\text{theo}} - \sigma_{\text{exp}})^2}{(\Delta\sigma_{\text{exp}})^2} \quad (13)$$

where σ_{theo} and σ_{exp} are the theoretical and experimental cross-sections, respectively, $\Delta\sigma_{\text{exp}}$ is the error variation of experimental cross-section and N expresses the total angle number.

3. RESULTS AND DISCUSSION

First nuclear potential, the WSP, has been acquired from the phenomenological WS potentials within the OM. The convenient values of the geometric parameters (r_v , r_w , a_v and a_w) of the WSP have searched. The r_v , r_w , a_v and a_w values have been evaluated as 1.08, 1.04, 0.74 and 0.91 fm, respectively. After the V_0 and W_0 values have been examined, the optical potential parameters have been listed in Table 1. Also, the χ^2/N values for the theoretical results of all the OM calculations have been calculated and given in Tables 1, 2 and 3.

Table 1. Optical potential parameters used in analysis with the WSP potential of ${}^7\text{Li} + {}^{159}\text{Tb}$ at various energies

E_{Lab} (MeV)	V_0 (MeV)	r_0 (fm)	a_0 (fm)	W_0 (MeV)	r_w (fm)	a_w (fm)	J_V (MeV.fm ³)	J_W (MeV.fm ³)	χ^2/N
24	93.0	1.08	0.74	9.50	1.04	0.91	188.7	18.1	0.67
26	71.0	1.08	0.74	9.80	1.04	0.91	144.0	18.6	2.67
28	53.5	1.08	0.74	10.1	1.04	0.91	108.5	19.2	5.88
30	100	1.08	0.74	28.5	1.04	0.91	202.8	54.2	3.21
35	50.0	1.08	0.74	35.3	1.04	0.91	101.4	67.1	0.24
40	49.0	1.08	0.74	36.3	1.04	0.91	99.4	69.0	5.04
44	34.0	1.08	0.74	36.8	1.04	0.91	69.0	70.0	0.26

Secondly, the real part of the optical potential has been generated with the DFM. For this, the calculations have been performed for the VMC, 2pF and HO densities of the ${}^7\text{Li}$ nucleus. The imaginary part has been based on the WS volume type potential. To get the agreement results with the experimental data, W_0 , r_w and a_w values of the imaginary potential have been investigated. In this way, it has been aimed to reduce the free parameter number of the imaginary potential. For this, while W_0 and a_w values are constant, the r_w value has been changed. Then, while W_0 and r_w are constant, the a_w value has been changed. Finally, for the r_w and a_w values, W_0 value has been researched. All the values obtained have been listed in Table 2.

Thirdly, the imaginary potential is replaced by the DF potential with a normalization factor. Thus, the free parameters are the normalization factors of real and imaginary potentials and the values are presented in Table 3.

Table 2. Optical potential parameters used in analysis with the $DF(R)$ potential for different densities of ${}^7\text{Li}$ at various energies

Density distribution	E_{Lab} (MeV)	N_R	W_0 (MeV)	r_w (fm)	a_w (fm)	J_V (MeV.fm ³)	J_W (MeV.fm ³)	χ^2/N
VMC	24	1.28	4.10	1.24	0.45	527.6	11.9	0.64
	26	0.88	10.5	1.24	0.45	362.4	30.4	2.50
	28	0.71	14.0	1.24	0.45	292.1	40.5	6.40
	30	1.22	14.5	1.24	0.45	501.5	42.0	5.14
	35	0.90	20.0	1.24	0.45	369.1	57.9	1.13
	40	1.00	24.0	1.24	0.45	409.1	69.5	7.84
	44	0.77	29.0	1.24	0.45	314.4	84.0	0.77
2pF	24	1.00	5.50	1.24	0.45	416.5	15.9	0.67
	26	0.73	16.5	1.24	0.45	303.7	47.8	2.50
	28	0.61	19.0	1.24	0.45	253.6	55.0	14.3
	30	1.09	19.5	1.24	0.45	452.7	56.4	5.23
	35	0.745	22.5	1.24	0.45	308.7	65.1	0.74
	40	0.69	25.0	1.24	0.45	285.2	72.4	7.00
	44	0.67	34.0	1.24	0.45	276.4	98.4	1.31
HO	24	1.25	5.00	1.24	0.45	515.5	14.5	0.72
	26	0.85	11.0	1.24	0.45	350.2	31.8	2.50
	28	0.66	12.0	1.24	0.45	271.6	34.7	6.72
	30	1.15	13.0	1.24	0.45	472.9	37.6	5.33
	35	0.82	16.5	1.24	0.45	336.4	47.8	1.51
	40	0.77	17.0	1.24	0.45	315.1	49.2	8.64
	44	0.70	30.5	1.24	0.45	285.9	88.3	1.42

Table 3. The normalization factors (N_R and N_I) used in analysis with the $DF(R+I)$

Density distribution	E_{Lab} (MeV)	N_R	N_I	J_V (MeV.fm ³)	J_W (MeV.fm ³)	χ^2/N
VMC	24	0.95	0.40	391.6	164.9	0.66
	26	0.30	0.30	123.5	123.5	2.68
	28	0.30	0.70	123.4	288.0	3.76
	30	1.10	1.25	452.2	513.8	1.94
	35	0.80	0.62	328.1	254.3	0.26
	40	1.00	1.00	409.1	409.1	3.28
	44	0.63	0.75	257.2	306.2	0.73
2pF	24	0.70	0.30	291.6	125.0	0.67
	26	0.50	0.32	208.0	133.1	2.87
	28	0.40	0.40	166.3	166.3	3.81
	30	0.80	0.85	332.3	353.0	2.16
	35	0.58	0.48	240.3	198.9	0.33
	40	0.75	1.10	310.0	454.7	3.60
	44	0.43	0.50	177.4	206.3	0.51
HO	24	0.95	0.40	391.8	165.0	0.66
	26	0.67	0.30	276.0	123.6	2.68
	28	0.51	0.40	209.9	164.6	4.30
	30	1.05	1.25	431.8	514.0	1.91
	35	0.75	0.60	307.7	246.1	0.35
	40	1.00	1.00	409.2	409.2	3.27
	44	0.66	1.00	269.6	408.4	1.60

Table 4. The cross-sections obtained with the WSP, DF(R) and DF(R+I) nuclear potentials in comparison with the literature

E_{Lab} (MeV)	WSP	$\sigma_{\text{DF(R)}}$			$\sigma_{\text{DF(R+I)}}$			$\sigma_{\text{Literature}}$
	(mb)	(mb)	(mb)	(mb)	(mb)	(mb)	(mb)	Ref. [5]
	WS	VMC	2pF	HO	VMC	2pF	HO	Ref. [5]
24	59.4	36.2	31.3	36.7	63.4	69.5	64.3	50
26	176.9	138.8	141.6	139.4	176.6	206.7	176.2	106
28	342.3	311.5	319.3	300.8	427.2	434.7	388.1	532
30	833.8	666.0	688.4	659.5	866.2	881.8	862.9	1008
35	1239.7	1020.0	1012.8	998.9	1178.4	1187.5	1170.5	1150
40	1576.2	1371.7	1317.0	1296.7	1636.0	1760.4	1641.3	1761
44	1752.7	1524.6	1539.0	1518.0	1732.4	1699.2	1811.9	1614

The theoretical results based on WSP as well as DF(R) and DF(R+I) with three different densities have been shown in Figures 2, 3, 4, 5, 6, 7 and 8 in comparison form. It has been observed that the results are in good agreement with the experimental data in general. At small energies such as 24, 26, 28 and 30 MeV, the evaluated data show a strong oscillation structure. As a result of this, it is very difficult to obtain a good convenient fit with the experimental data. To overcome this difficulty, we have adjusted the N_R and N_I values for each models, which are used to reproduce the elastic scattering data.

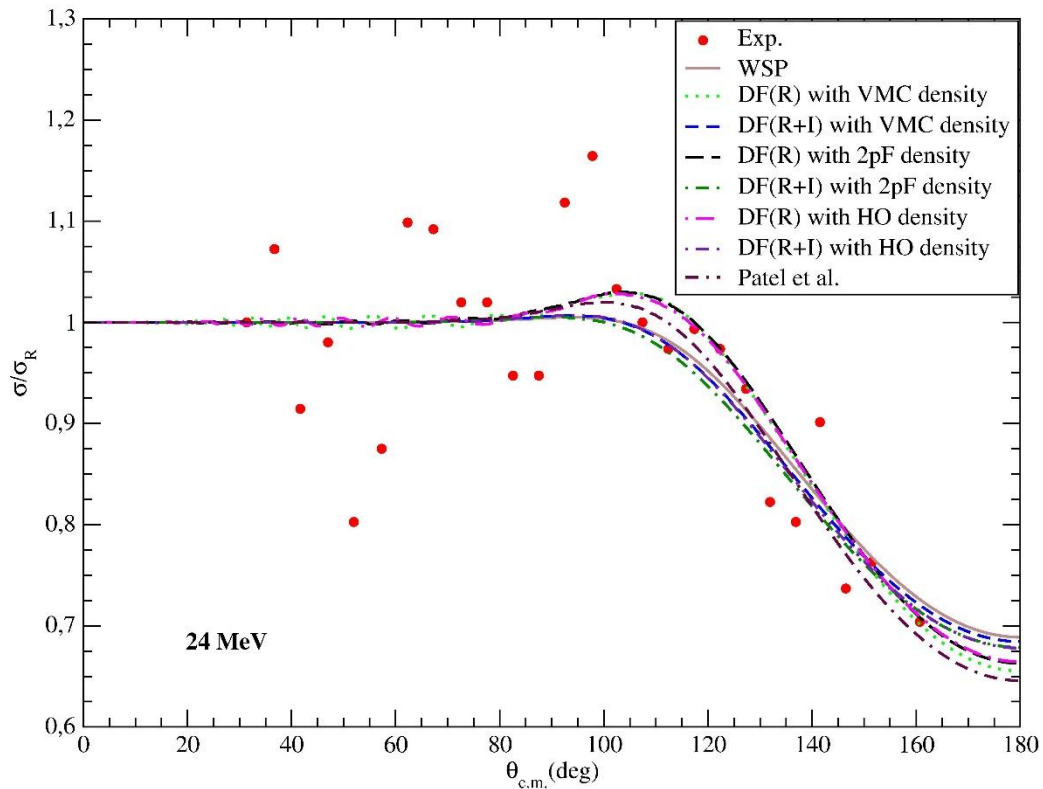


Figure 2. The elastic scattering cross sections obtained from optical model calculations employing the WSP, DF(R) and DF(R+I) potentials for different densities of ${}^7\text{Li}$ nucleus at 24 MeV in comparison with the literature

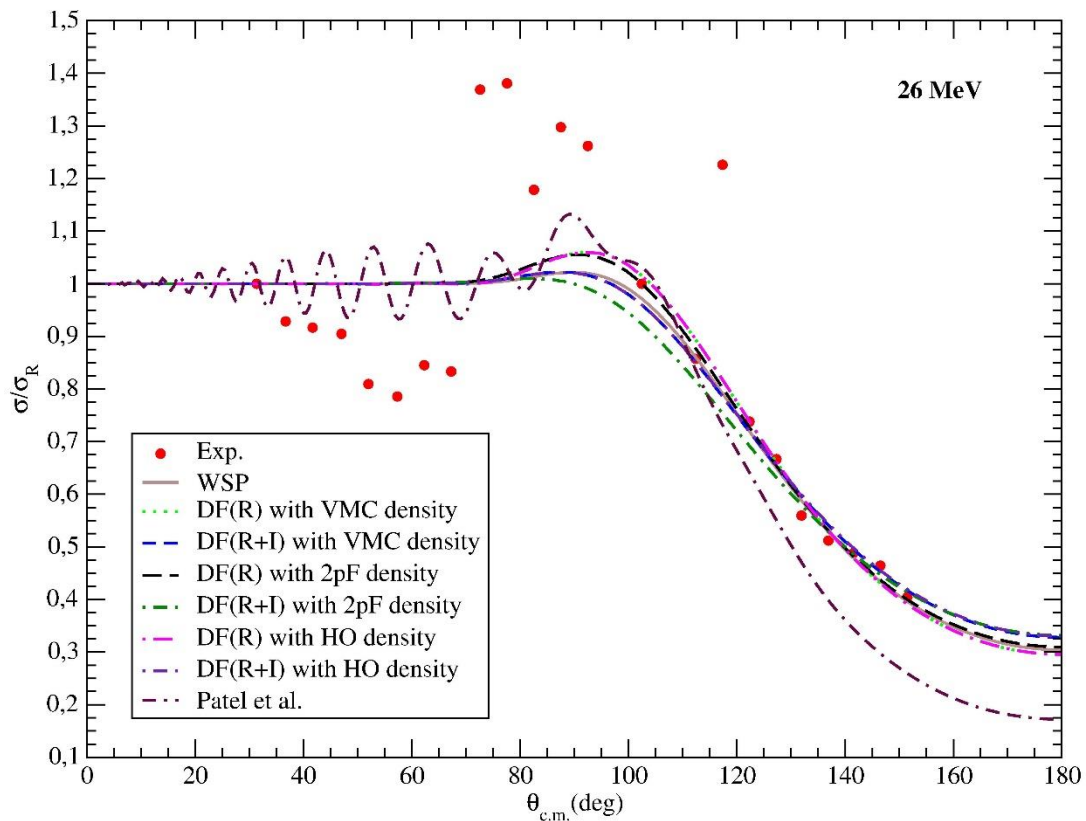


Figure 3. Same as in Figure 2, but for 26 MeV

These values have been listed in Table 2 for the DF(R) potential and in Table 3 for the DF(R+I) potential. In general, the DF(R+I) results with both VMC and 2pF density are slightly better than the other DF potentials investigated in this work. The N_R and N_I values in Table 3 change with a free parameter and it is difficult to obtain good results without changing the normalization factor. However, the N_R values in Table 2 change with the potential depth along with the r_w and a_w values. Thus, the fluctuation between the normalization values is less than the values of the normalization factors in Table 3. The change with the energy of the imaginary potential depths for the different densities used in the OM analysis of the $^7\text{Li} + ^{159}\text{Tb}$ reaction has been presented in Figure 9. It has been observed that the behavior of the potential depths is too similar to each other.

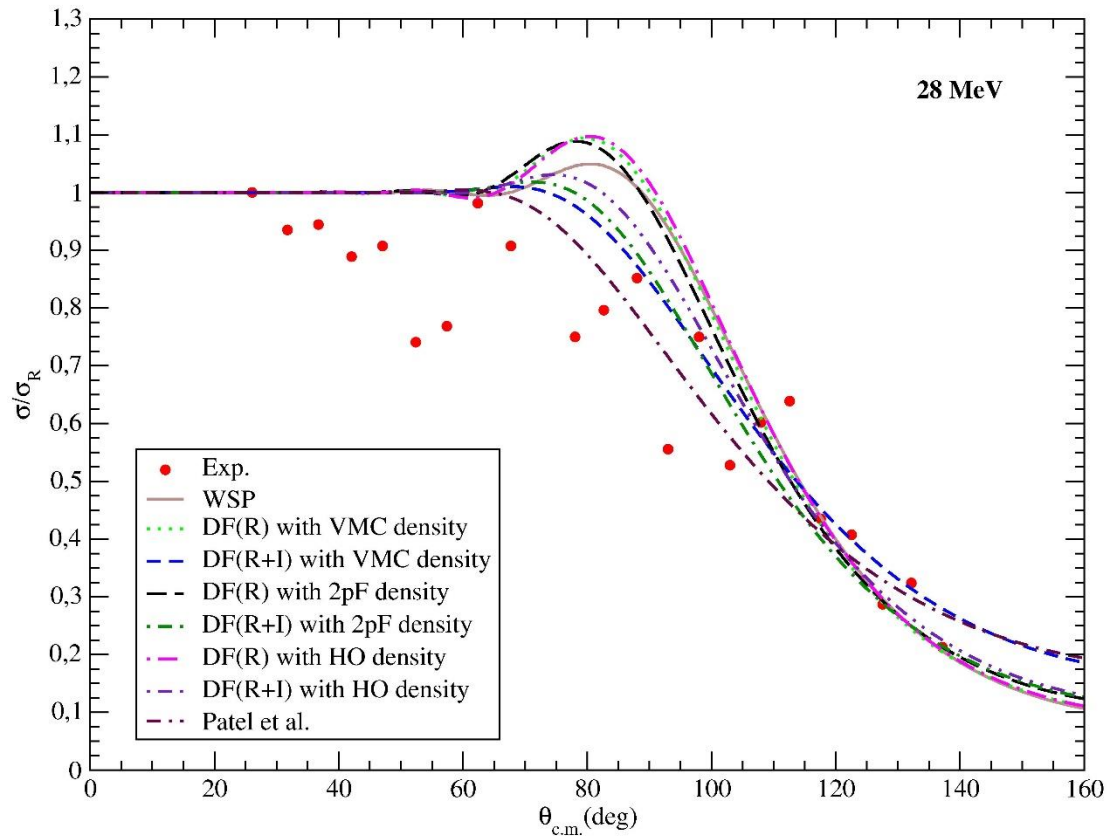


Figure 4. Same as in Figure 2, but for 28 MeV

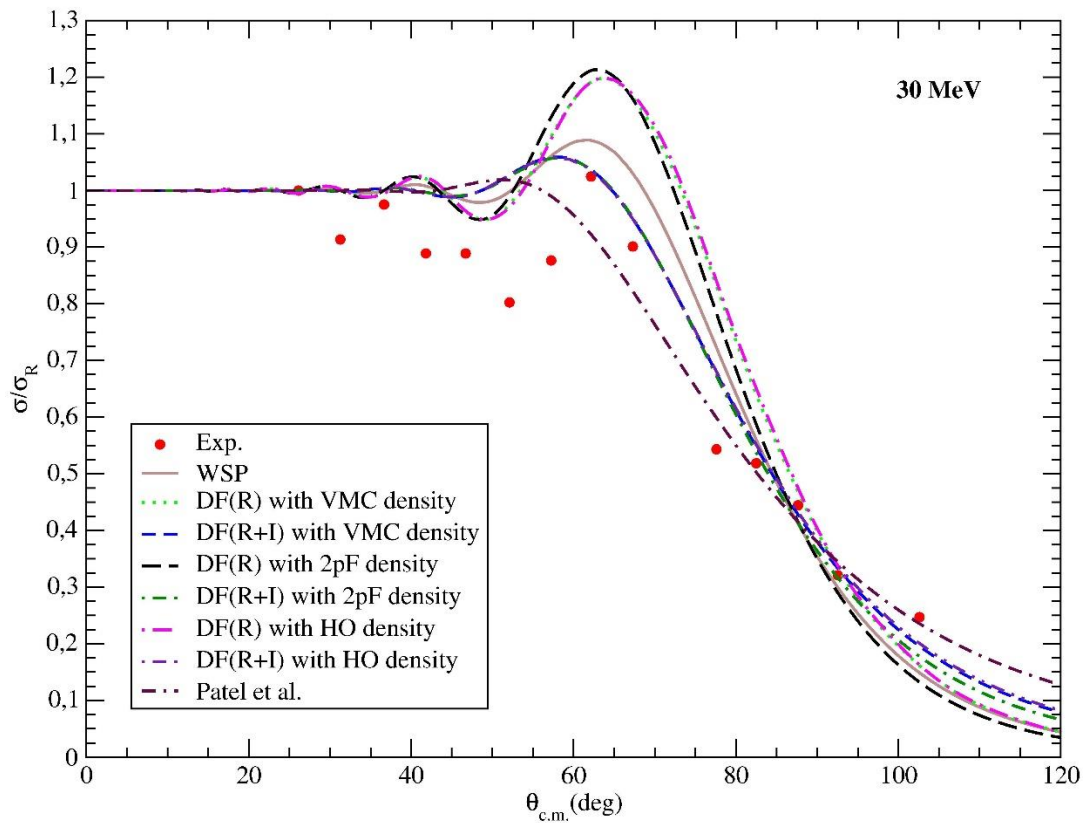


Figure 5. Same as in Figure 2, but for 30 MeV

Additionally, all the results of the WSP potential have been compared with the results of the previous study [5]. We have observed that the results with the WSP are better than the results of Patel et al. [5] at 26, 35 and 44 MeV. Also, we have obtained an energy dependence behavior for the imaginary part in the WSP calculations in contrast to the results of Patel et al. [5]. On the other hand, at 30 MeV, this behavior for the real part is broken.

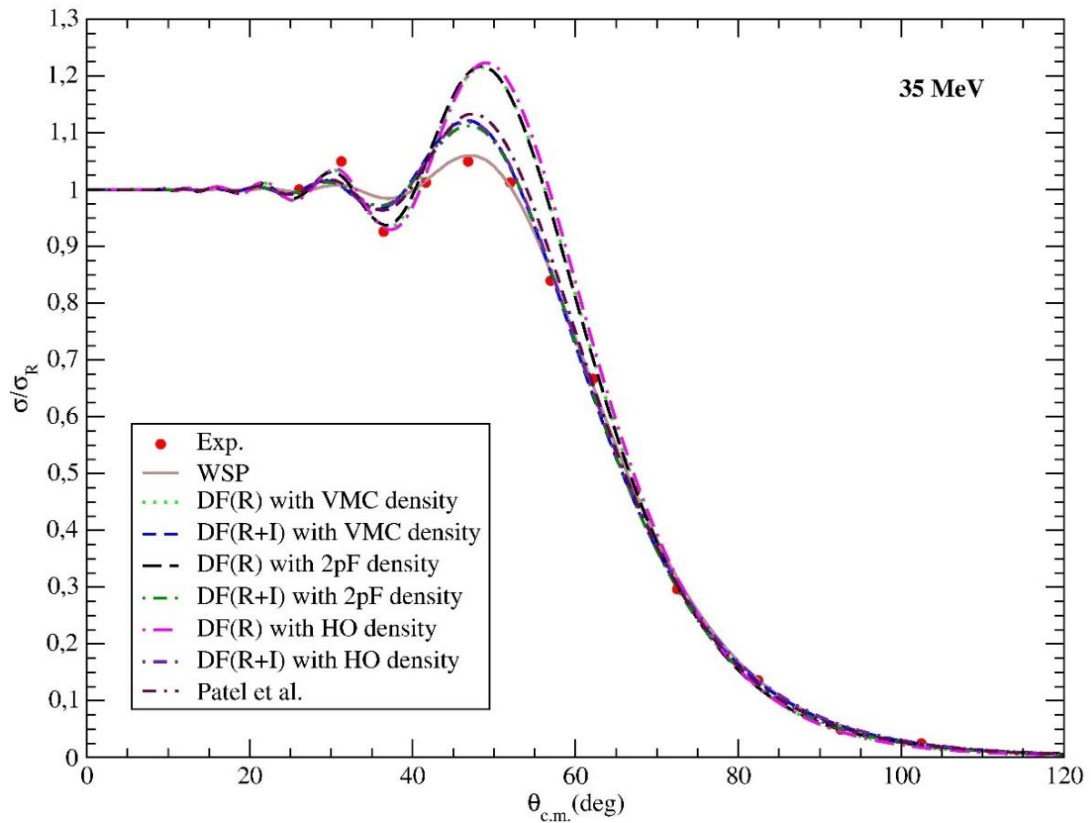


Figure 6. Same as in Figure 2, but for 35 MeV

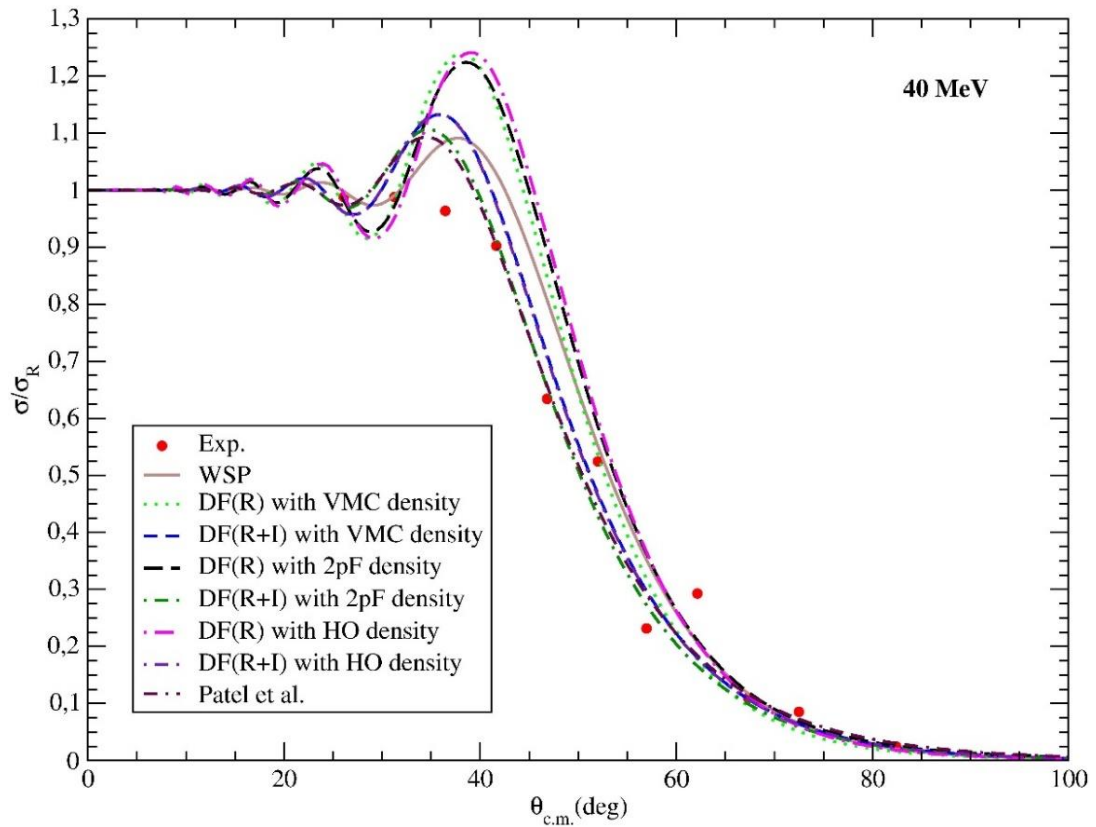


Figure 7. Same as in Figure 2, but for 40 MeV

In our study, we have obtained a simple equation for the imaginary potential which is dependent on the incident energy of the ${}^7\text{Li}$ nucleus. For this, we have found the average of three different depths of imaginary potential due to becoming three different imaginary potentials for three different densities. Then, we have derived a simple and useful equation for these new values of the imaginary potential. This equation is formulated as

$$W = -16.6 + 1.05E_{\text{Lab}} \quad (14)$$

where E_{Lab} is the incident energy of the ${}^7\text{Li}$ nucleus.

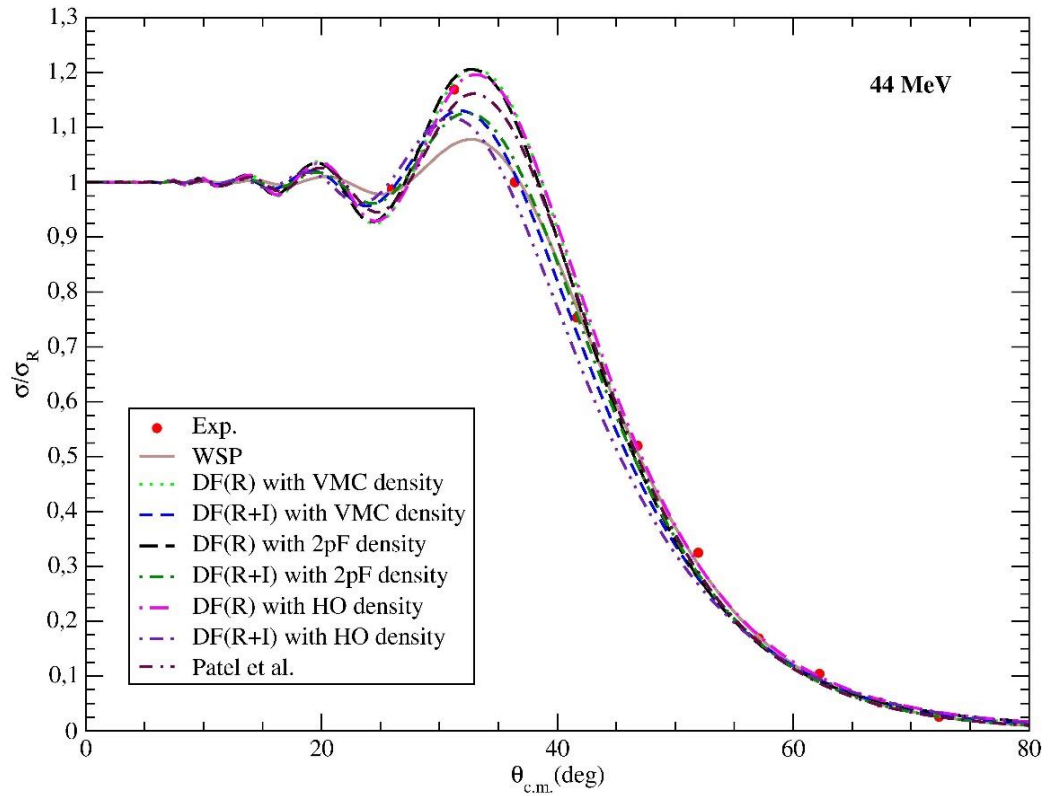


Figure 8. Same as in Figure 2, but for 44 MeV

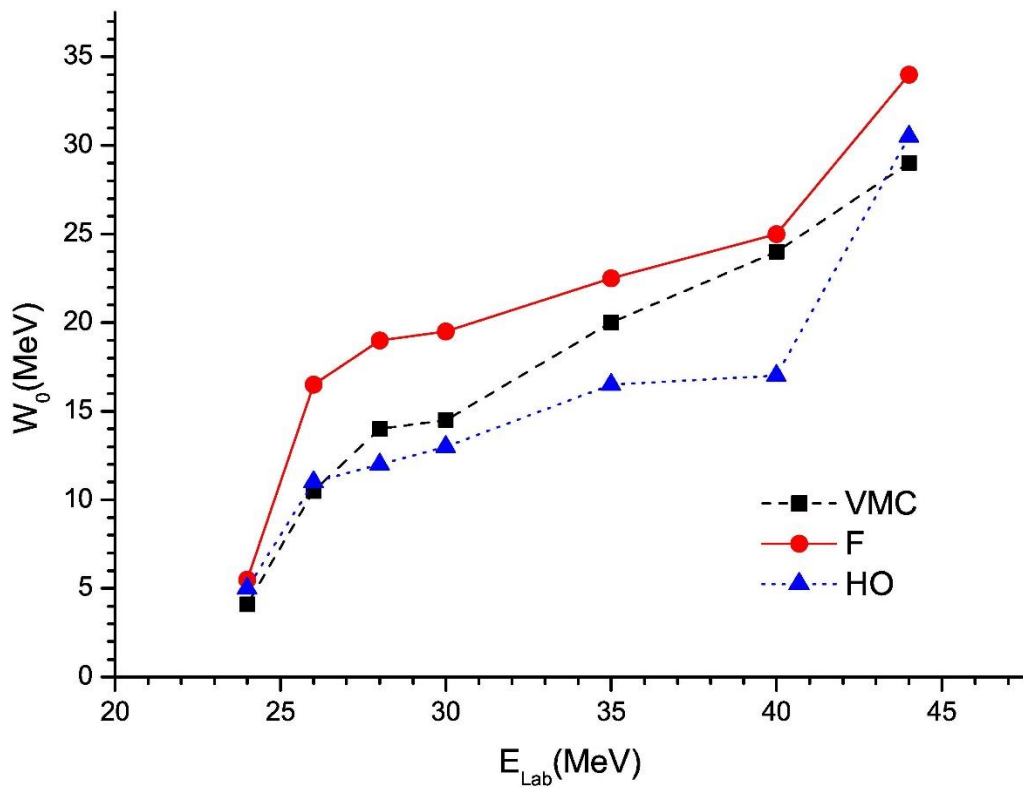


Figure 9. Energy dependence of the imaginary potential at various incident energies

In the OM analysis of a nuclear interaction, the optical potential parameters are organized with the volume integrals per interacting nucleon pair. The J_V and J_W volume integrals of all nuclear potentials have been listed in Tables 1, 2 and 3. It has been seen that the results are different substantially from each other. If the normalization (N_R) value is varied, the J_V values change. In this respect, by assuming the real potential form for the imaginary part listed in Table 3, the J_W values change with the N_I value. Whereas, the J_W values given in Table 2 change with the potential depth for the fixed r_w and a_w . Thus, the differences between the J_W values listed in Tables 2 and 3 have been observed.

In the present study, the cross-sections (σ) have been proved in comparison with the literature in Table 4. The change with the energy of the σ has been presented in Figure 10. When we have examined the results, we have noticed that the σ display the similar behavior with each other. That is, the σ increases with the incident energy. Also, the values of the σ are very close with each other. As well known, similar σ values for different OM calculations can be sent to agreement fits of the scattering data. Therefore, it can be said that a successful theoretical analysis of the data are achieved for different densities and potentials.

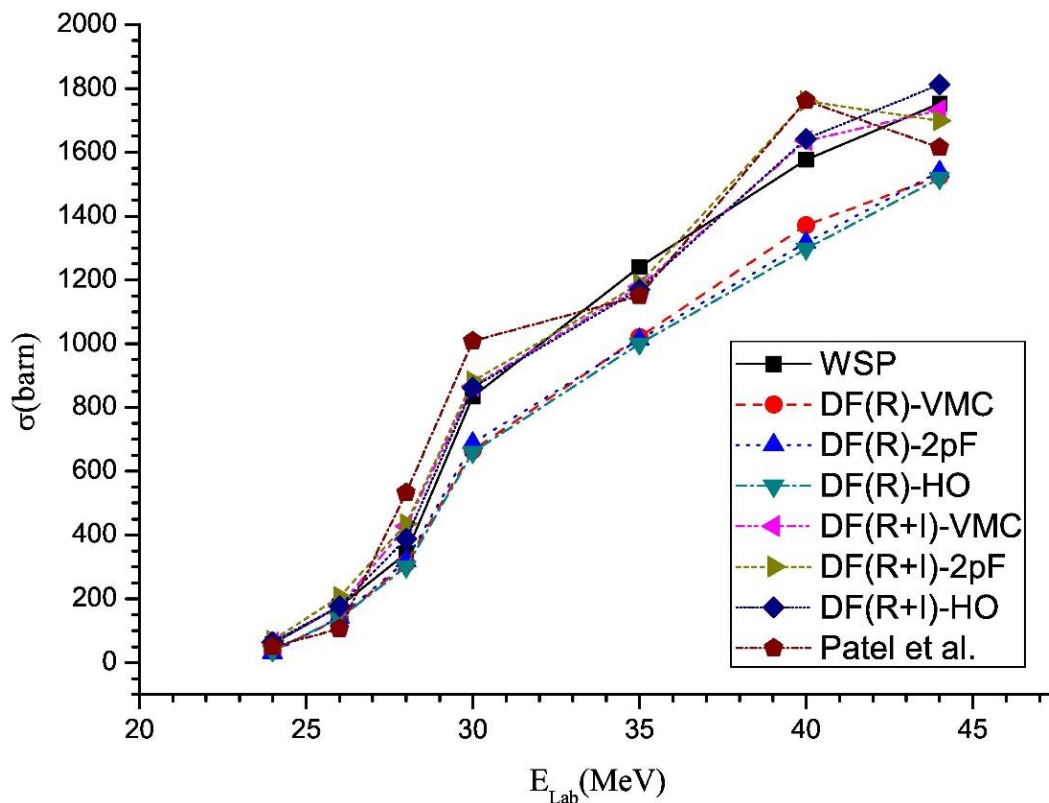


Figure 10. Energy dependence of the cross-sections obtained from the applied potentials at various incident energies

We have also derived a simple total reaction cross section (σ_R) equation for the average values of the reaction cross sections listed in Table 4. The equation is given by

$$\sigma_R(E_{Lab}) = (83.99E_{Lab} - 1925.83) \text{ mb} \quad (15)$$

Also, for comparison, the least-squares fit (Eq. 15) has been plotted by solid line in Figure 11.

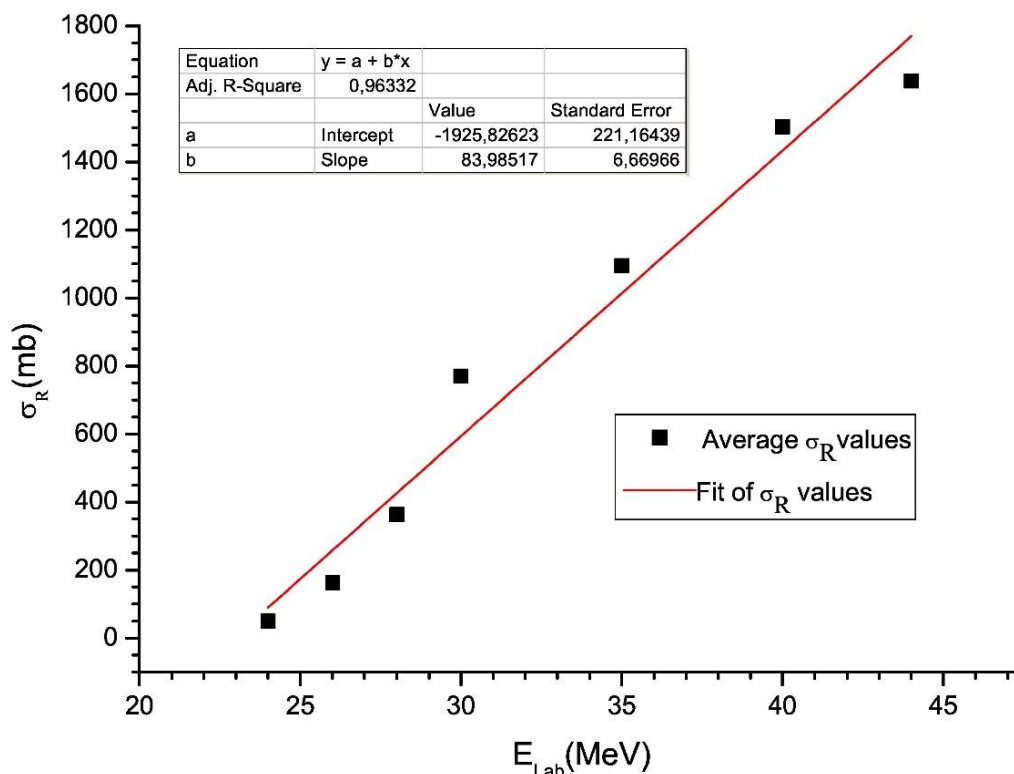


Figure 11. The energy dependence of the average σ_R values obtained by using DF(R) and DF(R+I) folded potentials for different densities. Solid line is the linear fit to the calculated values by Eq. 15

4. SUMMARY AND CONCLUSIONS

The angular distributions of the elastic scattering of the ${}^7\text{Li} + {}^{159}\text{Tb}$ reaction have been analyzed for different nuclear potentials at various incident energies. In this context, we have used the WSP potential as well as the DF(R) and DF(R+I) for three different densities of the ${}^7\text{Li}$ nucleus. We have determined the optical potential parameters given in tables for each systems. We have shown the theoretical results in figures. We have obtained consistent results with the experimental data although we have encountered difficulties due to the oscillating structure of the experimental data. Also, we have given J_V , J_W , σ and χ^2/N values. We have noticed that the σ values are in agreement with each other. The χ^2/N values are rather low which confirm the agreement between our results with the experimental data. Finally, new equations of ${}^7\text{Li} + {}^{159}\text{Tb}$ system have been obtained for both W and σ_R . The W and σ_R equations will be useful and practical in the theoretical calculations of the nuclear interactions.

CONFLICTS OF INTEREST

No conflict of interest was declared by the authors.

REFERENCES

- [1] Satchler, G.R. and Love, W.G., "Folding model potentials from realistic interactions for heavy-ion scattering", *Physics Reports*, 55:183-254, (1979).
- [2] Aygun, M., "Double-folding analysis of the ${}^6\text{Li} + {}^{58}\text{Ni}$ reaction using the ab initio density distribution", *European Physical Journal A*, 48:145, (2012).
- [3] Aygun, M., "A comprehensive analysis of different density distributions of neutron-rich ${}^{14}\text{Be}$ exotic nucleus", *Gazi University Journal of Science*, 29(2):263-272, (2016).

- [4] Aygun, M., Kucuk, Y., Boztosun, I. and Ibraheem, A.A., "Microscopic few-body and gaussian-shaped density distributions for the analysis of the ${}^6\text{He}$ exotic nucleus with different target nuclei", Nuclear Physics A, 848: 245-259, (2010).
- [5] Patel, D., Mukherjee, S., Biswas, D.C., Nayak, B. K., Gupta, Y.K., Danu, L. S., Santra, S. and Mirgule, E.T., "Investigation of the threshold anomaly for the ${}^7\text{Li} + {}^{159}\text{Tb}$ system", Physical Review C, 91:054614, (2015).
- [6] Satchler, G.R., Direct Nuclear Reactions, (Oxford University Press, Oxford) (1983).
- [7] Reference Input Parameter Library (RIPL-3), <http://www-nds.iaea.org/RIPL-3>.
- [8] Brandan, M.E. and Satchler, G.R., "The interaction between light heavy-ions and what it tells us", Physics Reports, 285:143-243, (1997).
- [9] Thompson, I.J., "Coupled reaction channels calculations in nuclear physics", Computer Physics Reports, 7:167-212, (1988).
- [10] Cook, J., "DFPOT - A program for the calculation of double folded potentials", Computer Physics Communications, 25:125-139, (1982).
- [11] Variational Monte Carlo (VMC) density distribution, <http://www.phy.anl.gov/theory/research/density/>.
- [12] Basak, A.K., Billah, M.M., Kobra, M.J., Sarkar, M.K., Mizanur Rahman, M., Pretam, K. Das, Hossain, S., Abdullah, M.N.A., Tariq, A.S.B., Uddin, M.A., Bhattacharjee, S., Reichstein, I. and Malik, F.B., "Non-monotonic potentials and vector analyzing powers of ${}^6,7\text{Li}$ scattering by ${}^{12}\text{C}$, ${}^{26}\text{Mg}$, ${}^{58}\text{Ni}$, and ${}^{120}\text{Sn}$ ", Europhysics Letters, 94:62002, (2011).
- [13] Vineyard, M.F., Cook, J., Kemper, K.W. and Stephens, M.N., "Optical potentials for the elastic scattering of ${}^6\text{Li} + {}^{12}\text{C}$, ${}^6\text{Li} + {}^{16}\text{O}$, and ${}^7\text{Li} + {}^{12}\text{C}$ ", Physical Review C, 30:916, (1984).